Author Accepted Manuscript (AAM)

Impaired M3 Muscarinic Acetylcholine Receptor Signal Transduction Through Blockade of Binding of Multiple Proteins to its Third Intracellular Loop

Dasiel O. Borroto-Escuela; Patricia A. Correia; Mileidys Perez Alea; Manuel Narvaez; Pere Garriga; Kjell Fuxe; Francisco Ciruela

Published article: Borroto-Escuela DO, Correia PA, Perez Alea M, Narvaez M, Garriga P, Fuxe K, Ciruela F. Impaired M3 Muscarinic Acetylcholine Receptor Signal Transduction Through Blockade of Binding of Multiple Proteins to its Third Intracellular Loop. Cellular Physiology and Biochemistry. 2010;25(4-5):397-408. doi:10.1159/000303044.

IMPAIRED M_3 MUSCARINIC ACETYLCHOLINE RECEPTOR SIGNAL TRANSDUCTION THROUGH BLOCKADE OF BINDING OF MULTIPLE PROTEINS TO ITS THIRD INTRACELLULAR LOOP

Dasiel O. Borroto-Escuela[a,c] *, Patricia A. Correia[b], Mileidys Perez Alea[c], Manuel Narvaez[d], Pere Garriga[c], Kjell Fuxe[a], Francisco Ciruela[e]

[a] Neuroscience Department, Karolinska Institutet, Stockholm, Sweden.

[b] W.M. Keck Centre for Integrative Neuroscience and Department of Physiology, University of California, San Francisco, USA.

[c] Centre for Molecular Biotechnology, Department of Chemical Engineering, Technical University of Catalonia, Barcelona, Spain.

[d] Department of Physiology, School of Medicine ,University of Málaga, Málaga, Spain

[e] Department of Pathology and Experimental Therapeutic, School of Medicine, Campus Bellvitge, IDIBELL-University of Barcelona, Barcelona, Spain.

*Corresponding author:

Retzius väg 8, Stockholm, Sweden. 17177.

Tel. +46 8 52487077, Fax: +46 8 315721

E-mail address: dasiel.borroto-escuela@ki.se (D.O. Borroto-Escuela).

Running head: Inhibitory effect of the third intracellular loop peptide.

Key words: third intracellular loop, muscarinic receptor, interacting proteins, G-protein coupled receptors, protein complexes.

ABSTRACT

Several motifs found in the third intracellular loop of the M_3 muscarinic receptor are critical for G protein activation and scaffold protein interaction. However, how multiprotein complexes form is not fully understood. A minigene encoding the third intracellular loop of the M_3 muscarinic receptor was constructed to explore whether peptides from this intracellular region could act as inhibitors of the muscarinic multiprotein complex formation and signaling. We found that this construct, when co-expressed with the M_3 receptor, has the ability to act as a competitive antagonist of G protein receptors and receptor-scaffold/accessory proteins. Transient transfection of human embryonic kidney-293 cells with DNA encoding the human M_3 and M_5 receptor subtypes results in a carbachol-dependent increase of inositol phosphate. Co-expression of the M_3 third cytoplasmic loop minigene dramatically reduces both carbachol-mediated G protein activation and inositol phosphate accumulation. Minigene expression also abrogates activation of M_3 and M_5 receptor mitogen-activated protein kinases pathway. Furthermore, minigene expression led to reduced AKT activation. These data, together with results of co-immunoprecipitation of different scaffold and kinase proteins, provide experimental evidence for the role for the third cytoplasmic loop of the human M_3 muscarinic receptor in G-protein activation and multiprotein complex formation.

INTRODUCTION

Muscarinic acetylcholine receptors (mAChRs) belong to a class I subfamily of heptahelical, transmembrane G-protein coupled receptors (GPCRs) and are represented by five distinct subtypes, denoted as M_1, M_2, M_3, M_4 and M_5 [1, 2] mAChRs signal through heterotrimeric guanine nucleotide-binding proteins (G-proteins), involving mainly the third intracellular loop (3ILoop). Muscarinic M_1, M_3 and M_5 receptors couple preferentially to the $G_{q/11}$ subunit type of G-proteins, activating phospholipase C-β, and inducing a subsequent increase in intracellular calcium concentration [3]. In contrast, M_2 and M_4 couple mainly to G-proteins of the $G_i/_o$ classes, typically leading to adenylate cyclase inhibition and activation of inward-rectifier potassium conductance [4, 5]. Among other possible responses, in a suitable cellular context, all mAChR subtypes can regulate a wide network of signaling intermediates, including small GTPase Rho, phospholipase D, phosphoinositide-3 kinase, nonreceptor kinases and mitogen-activated protein kinases [6-9].

Increasing evidence indicates that signaling efficiency/specificity for mAChRs is determined in part by accessory proteins that physically interact or are found in the microenvironment of

the receptor [10]. Several proteins have been shown to interact with mAChRs, including other GPCRs, kinases, and scaffold proteins such as β-arrestin [11, 12]. These proteins, along with classical core signaling entities (receptor, G protein and effectors), contribute to form a signalsome complex at the cytoplasmic face of the receptor [13]. Understanding the nature and features of such a complex may be a key step in designing novel strategies to develop next generation drugs. Sequence similarities of different receptor subtypes at the ligand binding sites is the main hurdle for designing and identifying proper subtype-selective ligands [14, 15]. However, important differences in size and sequence homology of the intracellular loops across different muscarinic receptors can be used to specifically identify each subtype. Previous studies using receptor-derived peptides from specific regions of the M_1 and M_2 receptors have shown the C-terminal tail of the 3ILoop is critical for receptor-G^-protein interaction [16] and the resulting signal transduction mediated by G proteins [17]. More recently, specific motifs in the 3ILoop of M_1 and M_3 receptors have been shown to bind some accessory proteins with high affinity (calmodulin, oncogenic SET protein, and small GTPase Rho) [12, 13, 18]. This experimental evidence points to a specific role of 3ILoop in receptor-G protein coupling, signal transduction and multiprotein complex formation. Thus, we hypothesized that the soluble expressed 3ILoop could act as a 3ILoop receptor analogue, competing with the receptor for its interacting proteins, and affecting the specific G-protein-mediated downstream effects.

To verify this hypothesis, we developed a minigene construct expressing the human M_3 muscarinic acetylcholine receptor 3ILoop (M_3R-3ILoop minigene), and evaluated its ability to affect downstream mAChRs signaling to $G_{q/11}$ proteins.

METHODS

Materials. Dulbecco's modified Eagle's medium, penicillin/streptomycin and fetal bovine serum were purchased from Invitrogen (Carlsbad, CA, USA). [^{35}S]-GTPγS (1,202 Ci/mmol), [^{3}H]-myo-inositol (3.0 Ci/ml) and N-[^{3}H]-methylscopolamine ([^{3}H]-NMS, 81 Ci/mmol), were from Amersham Biosciences (Piscataway, NJ, USA). Restriction enzymes were from New England Biolabs (Beverly, MA, USA). The rabbit anti-hemagglutinin (HA) polyclonal antibody (clone HA.11) was purchased from Covance (Berkeley, CA, USA). Carbamylcholine chloride (carbachol), atropine sulfate and all other reagents were purchased from Sigma-Aldrich (St. Louis, MO, USA). The pcDNA3-Flag-GRK2 encoding the bovine G receptor kinase-2 was kindly provided by Y. Chen (FUMC, Shanghai, China) and the

pcDNA3-Flag-CK1-α encoding the human casein kinase 1-α was kindly provided by M. Bini (Palermo University, Italy).

Plasmid constructs. The constructs presented here were made using standard techniques employing PCR and fragment replacement strategies. The cDNAs for the human M_3 and M_5 mAChRs (kindly provided by T. Bonner, NIH, USA and D. Bello, ETH, Switzerland, respectively) were subcloned into the mammalian expression vector pcDNA-3.1 (Invitrogen) containing three HA epitopes (gift from P. Calvo, SFU, CA, USA), thus resulting in the 3xHA-M_3R-pcDNA3.1 and 3xHA-M_5R-pcDNA3.1 vectors. Briefly, a 1.9 and 1.7 kb fragments encoding the human M_3R and M_5R were respectively amplified using sense and antisense primers harboring unique EcoRV and XbaI sites and then subcloned into EcoRV/XbaI sites of the mammalian pcDNA3.1-3xHA vector.

The cDNAs fragment encoding the entire third intracellular loop (3ILoop) of M_3 muscarinic acetylcholine receptor (Thr249-Ser495) was subcloned into the InterPlay® mammalian TAP system, pNTAP-B vector (Stratagene, La Jolla, CA, USA) resulting in the pTAP-M_3R-3ILoop vectors (M_3R-3ILoop minigene). The 3ILoop of M_3R was amplified from the 3xHA-M_3R-pcDNA vectors using the Expand High Fidelity PCR System (Roche, Basel, Switzerland) and subcloned into BamHI/EcoRI sites of the pNTAP-B vector.

Cell culture and transfection. HEK293T cells were maintained in Dulbecco's modified Eagle's medium supplemented with 10% fetal calf serum (FCS), 100 U/ml streptomycin, 100 µg/ml penicillin, 2 mM L-glutamine (all from Invitrogen) at 37°C in a humidified 5% CO_2 incubator. For transfections, 2×10^6 cells were seeded into 100-mm dishes. About 24 h later, cells were co-transfected with pTAP-M_3R-3ILoop vector and the corresponding human muscarinic plasmid, by using the Lipofectamine™ Plus reagent (Invitrogen). Cells were harvested 48 h after transfection and centrifuged at 30000xg for 30 min. Membrane fractions were frozen as aliquots in 5 mM phosphate buffer saline (PBS), pH 7.4, and stored at -80°C until required.

M_3R-3ILoop minigene transcript analysis. HEK293T cells were washed with PBS 48h post-transfection, and total RNA was purified using Quick Prep™ total RNA extraction kit (Amersham Biosciences) and subject to RT-PCR (Access RT-PCR system; Promega, USA). Primers were selected according to Gene Bank database (forward: 5'- GCG GAT CCA CTG GAG GAT CTA TAA GG-3'; reverse: 5'- GCG AAT TCG ACC AGG GAC ATC C-3) to amplify a segment of 541 bp. A RT-PCR negative control was performed loading DEPC water instead of cDNAs and a positive control was performed using G3DPH primers.

Membrane preparation and radioligand binding assay. About 48 h after transfection, HEK293T cells were washed twice with cold PBS, harvested and homogenized in binding buffer (25 mM HEPES, pH 7.4, 5 mM $MgCl_2$, 1 mM EDTA), using a Polytron tissue homogeniser. Cell membranes were collected by centrifugation at 20000xg for 15 min and homogenized as above. After centrifugation at 40000xg for 20 min at 4ºC, the final pellet was resuspended in binding buffer, and membranes were either used immediately or frozen in liquid nitrogen and stored at -80°C until needed. Protein concentration was determined by using the Bradford protein assay kit (Bio-Rad, Hercules, CA, USA). To determine the affinity of NMS for each sample, membranes were incubated with different concentrations of [^{3}H]-NMS (ranging from 12.5 pM to 1.5 nM) in 5 mM sodium phosphate (pH 7.4) containing 5 mM $MgCl_2$ at 25°C for 60 min. The incubations were stopped by filtration through Whatman (Maidstone, Kent, UK) GF/B filters and washed extensively with ice-cold PBS before scintillation counting. Nonspecific binding was determined in the presence of 10μM atropine.

Inositol phosphate determination. Transfected HEK293T cells were labeled for 18–24 h with [^{3}H]-myo-inositol (Amersham Biosciences) in DMEM (with glucose, w/o inositol (Invitrogen). After labeling, cells were washed and preincubated for 5 min in PBS at 37 °C, and subsequently incubated in FCS free medium with different concentrations of carbachol - or without carbachol- in the presence of 10 mM LiCl for 5 min. Reactions were stopped by perchloric acid addition. Inositol phosphates (IPs) were extracted and separated on Dowex AG1-X8 columns (Bio-Rad, Hercules, CA, USA). Total labelled IPs were then counted by liquid scintillation.

[^{35}S]-GTPγS binding assay. HEK293T cell membranes were diluted in an ice-cold buffer containing 10 mM HEPES and 0.1 mM EDTA, 5Mm deoxycholate (pH 7.4). Then pelleted and resuspended in a binding buffer consisting of 10 mM HEPES, 10 mM $MgCl_2$, and 100 mM NaCl (pH 7.4) at a final protein concentration of 125 μg/ml. Incubations were conducted in a final assay volume of 1 ml (125μg total protein) for 1 h at 30°C in the presence of 1 μM GDP and 0.3 nM [^{35}S]-GTPγS (Amersham Biosciences) and the suitable ligand concentration (carbachol from 1 nM to 1 mM). The reaction was stopped by addition of 5 ml of ice-cold buffer containing HEPES/NaOH (10 mM) (pH 7.4) and $MgCl_2$ (1 mM), immediately followed by rapid filtration through glass fibre filters GF/C filters (Whatman) presoaked in the same buffer. The filters were washed twice with 5 ml of buffer and the radioactivity was measured by scintillation counting. Nonspecific binding was determined in the presence of 10 μM GTPγS. Assays were performed in triplicate.

Co-immunoprecipitation and western blot. To immunoprecipitate the M_3 mAChR with its associated proteins, plasmids encoding the HA-M_3R receptor as well as the β-arrestin-GFP, Flag-GRK-2 or Flag-CK1-α expressing vectors were transiently co-transfected into HEK293T cells. 48 h later, cells were serum-deprived for 4 h., then incubated with vehicle or carbachol (20 μM) for 10 min and washed once with PBS before being solubilized for immunoprecipitation. Protein immunodetection on membranes was assessed using goat anti-M_3R antibody (1:1000; Santa Cruz Biotechnology, Santa Cruz, CA, USA), rabbit anti-HA polyclonal antibody (1:2000; Covance), mouse anti-flag M2 monoclonal antibody (1:5000; Sigma-Aldrich) and mouse anti-GFP monoclonal antibody (1: 10000; Novus Biological, Spain) as primary antibodies; and then horseradish-peroxidase (HRP) -conjugated goat anti-rabbit IgG (1:60000; Pierce, Rockford, IL, USA) or goat anti-mouse IgG (1:2000; Pierce, Rockford, IL, USA) as secondary antibody and developed using SuperSignal West Pico Chemiluminescent Substrate (Pierce).

MAPK and AKT assay. Co-transfected HEK293T cells expressing M_3 or M_5 receptor subtypes with or without the M_3R-3ILoop minigene were grown to 80% confluence and rendered quiescent by serum starvation overnight before MAPK or AKT phosphorylation assay. Subsequently, additional 2h incubation in fresh serum-free medium was performed to minimize basal activity. Then, cells were stimulated by adding medium containing the muscarinic agonist carbachol. Rapid rinsing, with ice-cold PBS finished stimulation, and then cell lysis was performed during 10 min by adding 500 μl ice-cold lysis buffer (50 mM Tris-HCL, pH 7.4, 150 mM NaCl, 1% TritonX-100, protease and phosphatase inhibitor cocktail). The cellular debris was removed by centrifugation at 13000xg for 5 min at 4°C, and the total protein content was measured using BCA Protein Assay Reagent (Pierce, Rockford, IL, USA). Aliquots corresponding to 5 μg of protein were mixed with sodium dodecyl sulfate (SDS) loading buffer, applied to 12% SDS-polyacrylamide gel electrophoresis (SDS-PAGE) and analyzed by Western blot. Extracellular signal regulated kinase 1/2 (ERK1/2) and protein kinase B (AKT) activation were assayed by incubating PVDF blots with a mouse antiphospho-ERK1/2 antibody (Sigma-Aldrich) and phospho-AKT antibody (New England Biolabs, UK) respectively. Control blots were also run in parallel and probed with rabbit anti-ERK1/2 antibody (Sigma-Aldrich), and total-AKT antibody that recognized both unphosphorylated and phosphorylated forms. The immunoreactive bands were visualized as described above and then measured by quantitative densitometry.

BRET assays. Forty-eight hours after transfection, HEK293T cells transfected with a constant amount (2 μg) of cDNA of M_3^{Rluc} and increasing amounts of cDNA of β-

arrestin^{GFP2}, were rapidly washed twice in PBS (4% glucose), detached, and resuspended in the same buffer. Cell suspension (40 µg of protein) was distributed in duplicated into 96-well microplates (either clear-bottomed or white opaque plates) for fluorescence and luminescence determinations). The total fluorescence of cell suspensions was quantified and then divided by the background (mock-transfected cells) in a POLARstar Optima plate reader (BMG, Labtechnologies, Offenburg, Germany) equipped with a high-energy xenon flash lamp, using a 10 nm bandwidth excitation filter of 400 nm and an emission filter of 510 nm. *Renilla luciferase*, total luminescence, was determined on samples incubated 10 min with 5-µM h-coelenterazine as described bellow. The background values for total luminescence were negligible, and they were subtracted from sample values.

For BRET measurement, 40 µg of cell suspensions were distributed in duplicate in 96-well white opaque microplates (Corning, NY) and incubated for 10 min at room temperature in the absence or presence of carbachol. DeepBlueC substrate (Molecular Probes, OR) was added at a final concentration of 5 µM, and readings were performed immediately after, using a POLARstar Optima plate-reader that allows the sequential integration of the signals detected with two filter settings [485 nm (440-500 nm) and 530 nm (510-560 nm)]. The ligand-induced BRET signal is calculated by subtracting the ratio of emission through the acceptor wavelength window over emission through the donor wavelength window for a vehicle-treated cell sample from the same ratio for a second aliquot of the same cells treated with ligand. With this calculation, the vehicle-treated cell sample represents the background, eliminating the requirement for measuring a donor-only control sample. Then, BRET ratio is defined as [(GFP^2 emission at 500–530)/(Rluc emission 440–500)] – cf., where cf. corresponds to (emission at 500–530)/(emission at 440–500) for the vehicle-treated cell sample in the same experiment.

Data analysis. All binding data were analyzed using the commercial program GraphPad PRISM 4.0 (GraphPad Prism, San Diego, CA, USA). Basal binding was defined as [^{35}S]-GTPγS binding without agonist in the [^{35}S]-GTPγS binding assay. For each agonist concentration, the percentage of binding over basal was calculated to determine the agonist-stimulated [^{35}S]-GTPγS binding. Data were fit to a sigmoidal dose-response curve. For statistical evaluation of the biochemical data, unless otherwise specified, one-way analysis of variance (ANOVA) was used followed by Tukey's Multiple Comparison post-test. *P* values less than 0.05 were considered significant.

RESULTS

Design, construction and expression of 3ILoop-minigene.

To determine whether the expression of the M_3-3ILoop peptide could function as an M_3R analogue, we generated a minigene vector that encodes the M_3R-3ILoop and a set of peptides (Calmodulin Binding Peptide/Streptavidin Binding Peptide (CBP/SBP)) as described in Materials and Methods (Fig. 1B). HEK293T cells were transiently co-transfected with the M_3R-3ILoop minigene and the M_3R mAChR . Total RNA was isolated 48 hours post-transfection and analyzed by RT-PCR, using a set of primers that spanned the vector (SBP) and inserted sequence (3ILoop), to confirm the transcription of the M_3R-3ILoop minigene. The presence of a single 541-base pair band corresponding to the RT-PCR product confirmed the transfection of cells with the minigene construct (Fig. 1C). To verify the expression of M3R-3ILoop peptide in the transfected HEK293T cells, 48 h post-transfection cells were also harvested and subjected to SDS-PAGE and western blot. A band of approximately 24 kDa molecular mass, corresponding to the expected mass of the designed I3Loop peptide, was identified in cells that have been transfected with the minigene construct.

Effect of M_3R-3ILoop minigene on receptor expression and ligand binding. The K_d values, for [^{3}H]-NMS binding to membranes, gained from cells expressing the M_3R in the presence and in the absence of the M_3R-3ILoop minigene were not significantly different (Table 1). It is also noticeable that the expression of the M_3R-3ILoop minigene did not alter the receptor density (B_{max} value) of the M_3R (Table 1).

HEK293T cells expressing M_5R mAChR were co-transfected with M_3R-3ILoop minigene to determine whether the M_3R-3ILoop protein had any effect on the thermodynamic properties of a related $G_{q/11}$-coupled receptor, the M_5R. Interestingly, M_5R showed similar specific [^{3}H]-NMS binding properties in the absence or presence of M_3R-3ILoop (Table 1). Overall, these results suggest that M_3R-3ILoop does not affect the conformational state of the orthosteric-binding site of M_3R and M_5R.

M_3R-3ILoop minigene inhibits agonist-mediated stimulation [^{35}S]-GTPγS binding. Since the 3ILoop of M_3R is known to be critical for G-protein coupling and activation [17], the expression of the M_3R-3ILoop minigene might compete for the same pool of G proteins by targeting the receptor-G protein boundary. Therefore, we tested whether the presence of the M_3R-3ILoop minigene, co-transfected in M_3 or M_5 transfected cells, had any effect on G-protein activation which was determined by measuring agonist-induced stimulation of [^{35}S]-GTPγS binding to membranes.The ability of carbachol to stimulated [^{35}S]-GTPγS binding

showed a similar maximal response (E_{max}) but different potency (pEC_{50}) when M3R and M5R were tested (pEC_{50}= 4.84 ± 0.04 and pEC_{50}= 5.77 ± 0.05, respectively; means ± S.D., n= 3, $p<0.05$) (Fig. 2).

Interestingly, co-expression of M_3R subtype with M_3R-3ILoop minigene resulted in a significant decrement in E_{max} (~45%) and 2.2 fold increased of pEC_{50} of the carbachol-mediated [^{35}S]-GTPγS binding, when compared with cells transfected with M_3R alone. We also found that cells expressing the M_5R subtype showed a similar M_3R-3ILoop minigene-mediated change in the agonist-stimulated [^{35}S]-GTPγS binding features (maximal response and potency) (Fig. 2).

To further test the specificity of the function of the 3ILoop of the M3 receptor to interact with cellular G proteins, we examined the ability of this peptide to modulate agonist-stimulation of specific [^{35}S]-GTPγS binding in cells heterologously expressing $G_{i/0}$-coupled dopamine D2-long (D_{2L}) receptor, as well as cells expressing $G_{S/olf}$ adenosine A_{2A} (A_{2A}) receptors. The addition of quinpirole (100nM) in cells expressing D_{2L} receptor or CGS 21680 (100nM) in cells expressing A_{2A} receptor, markedly induced an increase in [^{35}S]-GTPγS binding which was not affected by the expression of the M_3R-3ILoop minigene. These results suggest that M_3R-3ILoop minigene inhibits the $G_{q/11}$ protein-coupled mAChRs-mediated [^{35}S]-GTPγS binding in a specific manner.

Effect of 3ILoop-minigene Expression on PLC Activation.

We then analyzed agonist-stimulated Ins-(1,4,5)-P3 formation in HEK293T cells expressing each receptor subtype and either the minigene or an empty vector to assess whether the presence of the minigene could compete and recruit G protein-mediated activation of receptors. First, we characterized the time- and concentration-dependence of carbachol-stimulated [^{3}H]-myoinositolphosphate ([^{3}H]-myo-InsPs) accumulation in transfected M_3 and M_5-HEK293T cells. [^{3}H]-myo-InsPs accumulation reached a peak between 5-10 min after agonist exposure. Complete desensitization occurred within 30 min of high dose stimulation. Nonappreciable carbachol-stimulated [^{3}H]-myo-InsPs accumulation was detected in nontransfected cells (Figure not shown).

Fig. 2B shows the concentration-response curves for carbachol-dependent stimulation of [^{3}H]-myo-InsPs in M_3 and M_5-HEK293T cells co-expressing the minigene or the empty vector. Carbachol produced a seven-fold stimulation of inositol phosphate over basal levels, suggesting the presence of endogenous G proteins in HEK293 cells that can effectively

activate PLC. In contrast, expression of the minigene vector abolished M_3-agonist [^{3}H]-myo-InsPs accumulation at all agonist concentrations, with a decrease in relative efficacy in about 50%. A similar response was observed in cells expressing M_5 receptors. In this case, carbachol stimulation produced a 6-fold increase in [^{3}H]-myo-InsPs accumulation but co-expression of the minigene vector counteracts agonist stimulation (46% reduction in relative efficacy value compared with M5 receptor alone).

Besides the change observed in the maximum PLC response, there was a consistent and statistically significant reduction in the potency of carbachol to stimulate Ins-(1,4,5)-P3 release upon activation of the M3 or M5 receptor ($pEC_{50,}$ in the presence of M_3R-3ILoop minigene construct compared with the control, increased 3.1 ± 0.6 fold for the M_3 receptor and 3.4 ± 0.5 fold for the M_5 receptor).

To ensure that EC_{50} and E_{max} changes viewed were not due to changes in the receptor density, we plotted the negative logarithm of EC_{50} vs. receptor density for experiments with co-expression of the minigene. Although receptor expression was rather variable, EC_{50} shifts were independent of receptor density (data not shown).

Inhibition of ERK 1/2 and AKT activation is mediated by the expression of minigene construct. Previous experimental evidence supports the idea that at least two distinct mechanisms are involved in activation of ERK1/2 pathway by muscarinic receptors, PCK-dependent and/or state receptor phosphorylation dependent [19, 20]. As mentioned above, expression and ligand- binding capacity of M_3 and M_5 receptor subtypes were unaffected by the presence of minigene vector, whereas coupling to $G_{q/11}$ proteins was altered. Consequently, carbachol failed to stimulate phosphatidylinositol production. We evaluated whether the expression of minigene could further alter ERK1/2 signal transduction after agonist stimulation, and if this vector could be used as a potential inhibitor of this GPCR signaling.

First, a time course for ERK 1/2 activation was performed (Fig. 3A). Stimulation of both M_3 receptors co-transfected with empty vector or with minigene, by 20-μM carbachol, caused maximal activation of ERK1/2 at 5 min. However, fig. 3B shows that ERK1/2 activation by carbachol in cells co-transfected with the minigene was significantly lower than ERK1/2 activation in cells transfected with an empty vector (4–fold in less, $P<0.01$).

Fig. 3C shows the effects of minigene co-transfection on MAPK activity in cells expressing either M_3 or M_5 receptor subtypes. A significant decrease in ERK1/2 phosphorylation was observed in both cases when compared with activation in the absence of minigene vector.

Preincubation with the MEK specific inhibitor PD-98059 inhibited carbachol-induced ERK1/2 phosphorylation to the same extent as that obtained in cells co-transfected with the minigene construct. This confirmed that M_3R-3ILoop minigene vector acts as an efficient inhibitory protein of the MAPK signaling pathway after agonist stimulation.

Carbachol binding to the $G_{q/11}$ muscarinic receptors stimulates AKT-mediated cell growth and survival in many cell types [21]. Therefore, the effect of minigene expression on carbachol–induced AKT-activation was also studied.

Activating M_3 or M_5-expressing cells by carbachol incubation reaches a maximum of AKT phosphorylation at 10 min after stimulation. No activation occurred in cells pre-incubated with the PI3K antagonist LY294002 as shown in Fig. 4A-B. Western blot analysis revealed that, as previously noted in ERK1/2 signaling, co-transfection of M_3-or M_5-HEK293T with the minigene vector abolished the phosphorylation of AKT after agonist stimulation (Fig. 4A-B).

Modulation of receptor functions by sequestration of accessory proteins. Considering the dramatic decrease in ERK1/2 phosphorylation in cells expressing the minigene construct, we decided to analyze whether the minigene expression could modulate receptor function by sequestering receptor scaffold or accessory protein.

At least one of the two mechanisms described for MAPK activation by muscarinic receptor family could involve scaffold proteins, such as β-arrestin and kinases (GRK-2, GRK-3 and CK1-α), which form a direct complex with the receptor.

Co-immunoprecipitation experiments were carried out to discover if the direct complex formation had been altered or blocked by the presence of the cytoplasmatic 3ILoop. Fig. 5A shows co-immunoprecipitation data from HEK293T cells co-transfected with HA-M_3 receptor in the presence or absence of 3ILoop-M_3 minigene and each of the following vectors:β-arrestin-GFP2, Flag-GRK-2 and Flag-CK1-α.

Input levels of each protein and the efficiency of M_3 receptor immunoprecipitation were checked to ensure a balance between samples. In addition, we also analyzed the input level of immunoreactive M_3 receptor, β-arrestin-GFP, Flag-GRK-2 or Flag-CK1-α in original extracts as a positive control of each antibody quality (Fig. 5A, right lane). In all cases, low levels of immunoreactivity were associated with the receptor in basal conditions. However, preincubation of the cells with carbachol caused an increased association of each protein to the M3 receptor, as checked by densitometry of the immunoblots (Fig. 5B). Co-transfection with 3ILoop-M_3 minigene, as well as agonist preincubation, caused a decrease in

immunoreactivity for each protein to a level similar to that found under basal conditions. These low levels of co-immunoprecipitation probably resulted from the competition of the M_3R-3ILoop minigene with the same pool of proteins interacting with the receptor, thus blocking their association to the third intracellular loop. Co-immunoprecipitation results could also account for low signal levels gained in ERK ½ phosphorylation assays in the presence of the 3ILoop.

To determine whether sequestration of accessory proteins by the 3ILoop peptide affects their ability to modulate M3 receptor function, we used a BRET assay to determine if the 3ILoop peptide interferes with β-arrestin recruitment. B-arrestin has been shown to be particularly amenable to BRET analysis, and BRET has been used previously to investigate GPCR–β-arrestin and β-arrestin–ubiquitin interactions in parallel [22, 23]. The advantage of BRET compared with a number of other methods is that it is possible to observe interactions in living cells over time, in the presence of agonists and antagonists. We assayed carbachol-induced (1μM) interactions between M_3 receptor and β-arrestins-1 for 1 min pre-treatment and 120 min post-treatment (different intervals), observing a maximum BRET ratio between 5-20 min (data not shown). In addition, the ability of carbachol to stimulate BRET signal was tested in presence or absence of the 3ILoop. Co-expression of M_3^{Rluc} and β-arrestin^{GFP2} in presence of 3ILoop minigene led to a substantial reduction in BRET signal versus M_3^{Rluc} and β-arrestin^{GFP2} pair, as seen from the marked reduction of the BRET values (Fig. 6A). These results are consistent with those observed in western blot experiments (Fig 6B) and phosphorylation level determination (data not shown); where the presence of 3ILoop produced a dramatic decrease in β-arrestin binding and receptor phosphorylation upon agonist activation.

DISCUSSION

As part of an effort to define the potential role of the 3ILoop in protein-protein interactions and multiprotein complex organization, we report here the co-expression of a minigene construction that encoded the 3ILoop of the M_3 human muscarinic receptor with the intact receptor.

The rationale of this approach was to explore the ability of this structural determinant to interfere with G protein interaction or to compete for other interacting proteins that took part in a putative multiprotein complex formation. Our efforts were specifically focused on the 3ILoop of the M_3 muscarinic receptor subtype, because this region was reported to be

involved in direct G protein binding and activation, and the putative site for interaction of a group of scaffold or accessory proteins (arrestin binding, calmodulin and small G protein interactions) [24, 25]. Previous studies of cellular expression of fragments and in vitro G protein activation assays have reported the ability of the intracellular loops -or peptides derived from these loops- to interact with the same molecular partners as the intact receptor [26-28]. These experiments demonstrated that the 3ILoop domain of the M_3 receptor had a recognizable impact on the role of the intact M_3 receptor subtype. In our experiments events occurring at the plasma membrane were dramatically affected in cells co-expressing the 3ILoop minigene construct. Co-expressing the minigene construct with the wild-type receptor decreased G protein activation, phosphatidylinositol production, and subsequent signaling, without effecting normal ligand binding and receptor membrane expression. Our results showed that co-expression of the 3ILoop of the M_3 receptor with the M_5 subtype are similar to previous studies of the 3ILoop of the μ-opioid receptor, which altered the functionality of the intact μ-opioid receptor as well as other classes of GPCR [29].

While we only focused on the study of the effect of the 3ILoop, we cannot exclude the possible involvement of the first and second cytoplasmic loops or the C-terminal tail. Thus, although the 3ILoop is the largest intracellular loop, and is usually proposed to be one of the main sites for intracellular interaction, this does not exclude specific domains in other loops from playing a role in protein-protein interactions such as the formation of a multiprotein complex formation. In fact, the C-terminal tail is recognised to be an important structural determinant with antiapoptotic properties within the muscarinic receptor family [30] and the second intracellular loop, with the DRY motif, has also been described to bind the G protein[31].

In our experimental design, we chose to express the intracellular domain with two-epitope tags (CBP-SBP: TAP-system) at the N-terminal domain to purify the recombinant receptor. This will also allow us to develop further studies using mass spectrometry in order to discover the nature of the interacting proteins. The possibility of conformational and accessibility changes in potentially critical regions close to these tags was unlikely because of their small size (fewer than 15 aa). However, to ensure the proper construct was correctly incorporated into the cell, we used a RT-PCR strategy that involved primers spanning vector and insert sequences that would have been absent in the intact receptor construct.

We found that our minigene-system was able to reduce the mAchR-mediated G protein activation as much as 45%. These observations are consistent with those of other groups using a similar experimental approach with other GPCRs, such as δ-opioid, μ-opioid and α_2-

adrenergic receptors [29]. Upon co-expression of the minigene with the M_5 subtype, we also noted low affinity levels with agonist-stimulated [^{35}S]-GTPγS, and a decrease in efficacy. Overall, these experiments suggest that the minigene interferes with the specific function of the $G_{q/11}$ protein pool that couples with M_3 as well as with M_5 subtypes. Supporting this observation, we showed changes in the second messenger levels following expression of the minigene in intact cells. Agonist-mediated activation of Ins-(1,4,5)-P3 accumulation was blocked in the presence of the minigene, in cells expressing either M_3 or M_5 subtypes. Nevertheless, for M_5 subtype, the inhibitory effect of the 3ILoop was less pronounced. We also saw a decrease, not only in the maximal accumulation of phosphatidylinositol, but also in the potency of carbachol concentration-response curves, indicative of a reversible and competitive process. Our results are consistent with those previously reported for angiotensin receptor, where the presence of the second intracellular loop of angiotensin AT1a receptor resulted in a rise in the angiotensin II concentration needed for 50% stimulation for Ins-(1,4,5)-P3 release [32].

The low sequence homology within these receptors (at the level of 3ILoop) cannot account for the significant effect detected for the minigene impairment of receptor-G protein coupling process, suggesting that structural G-protein interaction sites are similar in both receptors [33]. This idea is consistent with the substantial reduction of Ins-(1,4,5)-P_3 production and G protein activation, which , however , did not decrease more than 50% with regard to the wild type. This indicates that multiple distinct structural domains could be involved in this interaction, as seen for dopamine and M_1 muscarinic receptors [16]. An alternative explanation is that the relevant domain that interacts with the G protein is exposed in the natural receptor, while the adapted minigene may not present or contain this structure, and therefore does not effectively compete for the binding with its homologous partner.

Several lines of evidence show that muscarinic receptors can activate the MAPK pathway in various ways, dependent on or independent of the classical G-protein activation pathway [20]. One of these mechanisms is PKC-dependent and is essential in ERK activation; it can involve βγ-subunits and $G_{\alpha q/11}$-subunits. Other mechanisms may depend more on the phosphorylation state, and are mediated by a group of different kinases, like GRK2/3 or CK1α, recruiting β-arrestin scaffold protein or other adapter proteins, respectively. Our experiments showed that cells co-expressing the minigene construct failed to phosphorylate ERK1/2 upon receptor activation, suggesting that PKC-dependent mechanism, as well as other mechanisms, which depend upon a group of kinases and accessory proteins, have been blocked.

In addition, using immunoprecipitation and bioluminescent assays, we analyzed whether the intact receptor, once activated, loses its ability to recruit and bind CK1α or β-arrestin in the presence of the minigene. This may help us understand whether the dramatic blockade of ERK1/2 phosphorylation observed involves the inhibitory effects of the minigene construct at the level of the G protein. Our immunoprecipitation and bioluminescent experiments showed a loss of CK1α and β-arrestin respectively, in the presence of the minigene in comparison with the wild type receptor. Taking this observation into consideration, one possible scenario is that the minigene construct not only disrupts the G subunit association, but also acts as an inhibitory or competitor subunit that potentially disrupts the multiprotein complex formation at the third intracellular loop, thus resulting in a markedly reduced ERK1/2 phosphorylation upon M3 receptor activation. Thus, the specific recruitment of accessory/scaffold proteins by the 3ILoop may be important for their ability to modulate M3 receptor function.

The M3 3ILoop is 256 residues long, containing multiple motifs of basic and acidic residues and some currently recognized functional sequence motifs. This primary sequence pattern is not conserved throughout the G protein-coupled receptor superfamily, and not even within the class A rhodopsin-like receptor subfamily that represents the closest structurally related class of GPCRs. This may eventually form a conformational structural motif that will be more broadly representative and determine part of the specificity for each receptor in these families. However, no structural data are available to confirm or refute this hypothesis.

Interacting proteins for such motifs appearing in a modular form can be identified by affinity purification approaches, such as yeast two-hybrid screening and immunoprecipitation. Our current work, in which the minigene construct representing the 3ILoop of the M_3 muscarinic receptor specifically influences the intracellular signaling of the intact receptor, probably blocking putative multiprotein complex formation, supports the notion that important motifs could be present in this region. The fact that this loop is long could make it an ideal tool for exploring potential molecular partners that might mediate the observed effect under different cellular conditions. The use of a TAP-system strategy that complements the co-expression experiments of the construct with the intact receptor under different physiological conditions would be a productive approach to study protein-protein interactions, not only for muscarinic receptors but also for other types of GPCR.

In summary, our results suggest that the presence of the M_3R-3ILoop minigene construct not only prevents G-protein coupling to M_3 receptors, but also impairs coupling of other GPCRs that selectively interact with the same G protein population ($G_{q/11}$).We found that the minigene construct can inhibit the M_3 muscarinic acetylcholine signal transduction pathway

and its functionality, probably by recruiting M_3R interacting proteins as confirmed by co-immunoprecipitation and bioluminescent experiments. These results highlight the functional relevance of the interplay among GPCRs and selective G-protein pools, a key process for cell regulation. Furthermore, muscarinic receptor-derived peptides could be used as selective inhibitors for protein-protein interaction, this may be useful for developing a novel pharmacological strategies.

ACKNOWLEDGMENTS

This study was supported by the Ministerio de Ciencia e Innovación, Gobierno de España (Grants SAF2005-0848-C04-02 and SAF2002-0345-C0302 to P.G.; and SAF2008-01462 and CSD2008-00005 to F.C.); by European Social Foundation and Gobierno de Catalunya (FI2004-BE2006 to D.O.B-E); and from the Swedish Research Council (04X-715), Torsten and Ragnar Söderberg Foundation to KF. F.C belongs to the "Neuropharmacology and Pain" accredited research group (Generalitat de Catalunya, 2009 SGR 232). We infinitely appreciate the assistance and comments provided by Margaret Carr during correction of the manuscript.

REFERENCES

1 Caulfield MP, Birdsall NJ: International union of pharmacology. Xvii. Classification of muscarinic acetylcholine receptors. Pharmacol Rev 1998;50:279-290.
2 Ishii M, Kurachi Y: Muscarinic acetylcholine receptors. Curr Pharm Des 2006;12:3573-3581.
3 Nahorski SR, Tobin AB, Willars GB: Muscarinic m3 receptor coupling and regulation. Life Sci 1997;60:1039-1045.
4 Yamada M, Inanobe A, Kurachi Y: G protein regulation of potassium ion channels. Pharmacol Rev 1998;50:723-760.
5 Volpicelli LA, Levey AI: Muscarinic acetylcholine receptor subtypes in cerebral cortex and hippocampus. Prog Brain Res 2004;145:59-66.
6 Schmidt M, Rumenapp U, Keller J, Lohmann B, Jakobs KH: Regulation of phospholipase c and d activities by small molecular weight g proteins and muscarinic receptors. Life Sci 1997;60:1093-1100.
7 Kozma R, Sarner S, Ahmed S, Lim L: Rho family gtpases and neuronal growth cone remodelling: Relationship between increased complexity induced by cdc42hs, rac1, and acetylcholine and collapse induced by rhoa and lysophosphatidic acid. Mol Cell Biol 1997;17:1201-1211.
8 Linseman DA, Heidenreich KA, Fisher SK: Stimulation of m3 muscarinic receptors induces phosphorylation of the cdc42 effector activated cdc42hs-associated kinase-1 via a fyn tyrosine kinase signaling pathway. J Biol Chem 2001;276:5622-5628.
9 Firth TA, Jones SV: Gtp-binding protein gq mediates muscarinic-receptor-induced inhibition of the inwardly rectifying potassium channel irk1 (kir 2.1). Neuropharmacology 2001;40:358-365.

10 Eglen RM: Muscarinic receptor subtypes in neuronal and non-neuronal cholinergic function. Auton Autacoid Pharmacol 2006;26:219-233.
11 van Koppen CJ, Kaiser B: Regulation of muscarinic acetylcholine receptor signaling. Pharmacol Ther 2003;98:197-220.
12 Simon V, Guidry J, Gettys TW, Tobin AB, Lanier SM: The proto-oncogene set interacts with muscarinic receptors and attenuates receptor signaling. J Biol Chem 2006;281:40310-40320.
13 Borroto-Escuela DO, Ciruela F: Muscarinic receptor-associated proteins: More than just an interaction between proteins. Nova Science Publishers, 2007.
14 Adem A, Karlsson E: Muscarinic receptor subtype selective toxins. Life Sci 1997;60:1069-1076.
15 Nelson CP, Challiss RA: "Phenotypic" Pharmacology: The influence of cellular environment on g protein-coupled receptor antagonist and inverse agonist pharmacology. Biochem Pharmacol 2007;73:737-751.
16 Hawes BE, Luttrell LM, Exum ST, Lefkowitz RJ: Inhibition of g protein-coupled receptor signaling by expression of cytoplasmic domains of the receptor. J Biol Chem 1994;269:15776-15785.
17 Liu J, Blin N, Conklin BR, Wess J: Molecular mechanisms involved in muscarinic acetylcholine receptor-mediated g protein activation studied by insertion mutagenesis. J Biol Chem 1996;271:6172-6178.
18 Zhang Y, Wang D, Sadee W: Calmodulin interaction with peptides from g-protein coupled receptors measured with s-tag labeling. Biochem Biophys Res Commun 2005;333:390-395.
19 Budd DC, McDonald JE, Tobin AB: Phosphorylation and regulation of a gq/11-coupled receptor by casein kinase 1alpha. J Biol Chem 2000;275:19667-19675.
20 Budd DC, Willars GB, McDonald JE, Tobin AB: Phosphorylation of the gq/11-coupled m3-muscarinic receptor is involved in receptor activation of the erk-1/2 mitogen-activated protein kinase pathway. J Biol Chem 2001;276:4581-4587.
21 Cui QL, Fogle E, Almazan G: Muscarinic acetylcholine receptors mediate oligodendrocyte progenitor survival through src-like tyrosine kinases and pi3k/akt pathways. Neurochem Int 2006;48:383-393.
22 Perroy J, Pontier S, Charest PG, Aubry M, Bouvier M: Real-time monitoring of ubiquitination in living cells by bret. Nat Methods 2004;1:203-208.
23 Kocan M, Pfleger KD: Detection of gpcr/beta-arrestin interactions in live cells using bioluminescence resonance energy transfer technology. Methods Mol Biol 2009;552:305-317.
24 Keller J, Schmidt M, Hussein B, Rumenapp U, Jakobs KH: Muscarinic receptor-stimulated cytosol-membrane translocation of rhoa. FEBS Lett 1997;403:299-302.
25 Novi F, Stanasila L, Giorgi F, Corsini GU, Cotecchia S, Maggio R: Paired activation of two components within muscarinic m3 receptor dimers is required for recruitment of beta-arrestin-1 to the plasma membrane. J Biol Chem 2005;280:19768-19776.
26 Gilchrist A, Li A, Hamm HE: Design and use of c-terminal minigene vectors for studying role of heterotrimeric g proteins. Methods Enzymol 2002;344:58-69.
27 Abdulaev NG, Ngo T, Chen R, Lu Z, Ridge KD: Functionally discrete mimics of light-activated rhodopsin identified through expression of soluble cytoplasmic domains. J Biol Chem 2000;275:39354-39363.
28 Hayashida W, Horiuchi M, Dzau VJ: Intracellular third loop domain of angiotensin ii type-2 receptor. Role in mediating signal transduction and cellular function. J Biol Chem 1996;271:21985-21992.

29 Morou E, Georgoussi Z: Expression of the third intracellular loop of the delta-opioid receptor inhibits signaling by opioid receptors and other g protein-coupled receptors. J Pharmacol Exp Ther 2005;315:1368-1379.
30 Tobin AB, Budd DC: The anti-apoptotic response of the gq/11-coupled muscarinic receptor family. Biochem Soc Trans 2003;31:1182-1185.
31 Blin N, Yun J, Wess J: Mapping of single amino acid residues required for selective activation of gq/11 by the m3 muscarinic acetylcholine receptor. J Biol Chem 1995;270:17741-17748.
32 Thompson JB, Wade SM, Harrison JK, Salafranca MN, Neubig RR: Cotransfection of second and third intracellular loop fragments inhibit angiotensin at1a receptor activation of phospholipase c in hek-293 cells. J Pharmacol Exp Ther 1998;285:216-222.
33 Burstein ES, Spalding TA, Brann MR: Structure/function relationships of a g-protein coupling pocket formed by the third intracellular loop of the m5 muscarinic receptor. Biochemistry 1998;37:4052-4058.

FIGURE LEGENDS

Fig. 1. Minigene design and topological model of the M_3 receptor. (A) A two-dimensional topology of the M_3 human muscarinic receptor sequence is represented (extracellular space at the top and the intracellular space at the bottom). Filled circles represent the amino acid sequence of peptide 3ILoop employed to construct the minigene. (B) Design of the M_3R-3ILoop minigene vector (884 bp) is also depicted: CBP, Calmodulin Binding Peptide; SBP, Streptavidin Binding Peptide; 3ILoop (630 bp), the Third Intracellular Loop of the M_3 human muscarinic receptor. (C) HEK 293 cells were transiently co-transfected with M_3 or M_5 receptor subtypes and M_3R-3ILoop minigene vector. To confirm the transiently transfection of minigene in HEK 293 cells, total RNA was isolated and subjected to RT-PCR. The PCR analysis was achieved using primers specific for a CBP + 3ILoop fragment. Separation of the PCR products on 1.5% agarose gels shows the presence of the M_3R-3ILoop minigene RNA by a single 541-bp band. Lane 1 is a 1-kilobase pair DNA ladder; lane 2 is a PCR product from cells transfected with pcDNA-3xHA-M_3; lane 3 corresponds to cells co-transfected with pcDNA-3xHA-M_3 and M_3R-3ILoop minigene; lane 4 corresponds to cells transfected with

pcDNA-3xHA-M_5; and lane 5, to cells co-transfected with pcDNA-3xHA-M_5 and 3ILoop-M_3 minigene. G3DPH gene was used as housekeeping control.

.

Fig. 2. (A) The 3ILoop-minigene inhibit agonist-stimulated [^{35}S]-GTPγS binding on cells expressing the M_3 and M_5 receptor subtypes. [^{35}S]-GTPγS (0.3 nM) binding to membranes prepared from transiently expressing M_3-HEK293T or M_5-HEK293T cells was measured after incubation at different concentrations of carbachol (CCh) for 1h at 30°C in the presence or absence of M_3R-3ILoop minigene (5μg). Values are expressed as percentage (%) of specific binding to the sample without ligand (control). Data are means ± S.D. from a representative experiment preformed in triplicate. (B) Results of 3ILoop-minigene vector and muscarinic receptor subtypes co-expression on PLC activity in CCh-stimulated HEK293T cells. Cells cotransfected with M_3 or M_5 receptor subtypes and M_3R-3ILoop minigene or empty vector were stimulated with CCh as showed, for 1 hr at 37°C in presence of LiCl as described in "Materials and Methods". Data are presented as increase of InsPs (DPM) above basal levels in the presence of carbachol. Basal levels viewed with the various receptors were not significantly different. Data represent the average ± S.E.M. values of triplicate determinations of three independent experiments.

Fig. 3. Expression of the 3ILoop-minigenes inhibit agonist-mediated ERK ½ phosphorylation. (A) Time-dependent course of ERK1/2 activation on CCh-stimulated M_3-HEK293T cells transfected or not with M_3R-3ILoop minigene. Cells were incubated with 1 mM of CCh for the showed time points. (B) Densitometry analysis of time course of ERK1/2 activation following CCh exposure is shown. Phosphorylation was quantified by scanning densitometry using the NIH Image program and normalized against total ERK1/2 protein. Means ±S.E.M are shown; n= 6. *Significantly different compared with M_3-15min (ANOVA:

$p<0.05$); **Significantly different compared with M_3-5min (ANOVA: $p<0.01$). (C) Western blot analysis for phospho-ERK1/2 (p-ERK) following incubation with 1 mM of carbachol for 5 min. In HEK293T cells transiently expressing M_3 or M_5, co-transfected with the M_3R-3ILoop minigene (5μg) (lanes 4 and 6 respectively) or empty vector (lanes 3 and 5). M_3-HEK293T cells, nonstimulated with carbachol (lane 1) and carbachol-stimulated M_3-HEK293T in the presence of MAPK specific inhibitor PD-98059 (lane 2), were analyzed as internal control samples. Equal loading was confirmed with antibodies against total ERK1/2.

Fig. 4. 3ILoop effect on AKT phosphorylation mediated upon muscarinic receptor activation. (A) HEK293T cells co-transfected with each receptor subtype and the M_3R-3ILoop minigene (lanes 4 and 6 respectively) or empty vector (lanes 3 and 5) were exposed to 1 mM CCh for 10 min after 48 h of transfection. Cell lysates were resolved by SDS-PAGE (12%) and Western blots performed with an antibody against phosphorylated AKT. Nonstimulated M_3-HEK293T cells (lane 1) and CCh-stimulated M_3-HEK293T in the presence of a selective PI3K inhibitor, LY294002 (lane 2) were assayed as internal controls. Equal loading was confirmed with rabbit anti-AKT antibody (New England Biolabs, UK). (B) The extent of AKT phosphorylation was quantified by scanning densitometry. Means ±S.E.M is shown; n= 4. **Significantly different compared with M_3 (ANOVA: $p<0.01$). ##Significantly different compared with M_5 (ANOVA: $p<0.01$).

Fig. 5. Modulation of scaffold proteins association by co-expression of 3ILoop. (A) HEK293T cells co-transfected with M_3 receptor, in the presence or absence of the M_3R-3ILoop minigene, plus each of the following proteins, β-arrestin-GFP, Flag-GRK-2 or Flag-CK1-α), were stimulated with CCh before solubilization. Extracts were immunoprecipitated with anti-HA antibody (or nonimmune IgG control) before Western blotting. At the top

sections, the immunoprecipitation was probed with an antibody against the M_3 muscarinic receptor (goat anti-M_3R antibody, 1:1000; Santa Cruz Biotechnology). The middle sections show specific co-immunoprecipitation with β-arrestin-GFP (mouse anti-GFP monoclonal antibody, 1: 10000; Novus Biological). A low-level of specific pulldown of β-arrestin-GFP can be seen when cells are co-expressed with the 3ILoop minigene construct. Similar effects were remarked in the bottom sections when immunoprecipitations were probed with anti-FLAG antibody for both kinases (GRK-2 and CK1-α) under the same conditions (mouse anti-flag M2 monoclonal antibody, 1:5000; Sigma-Aldrich). The right panel (positive control) represents the input levels of immunoreactive M_3 receptor, β-arrestin-GFP, Flag-GRK-2 or Flag-CK1-α in original extracts. Interacting protein co-immunoprecipitated was normalized for immunoprecipitated 3xHA-M_3 receptor. Blots are representative of at least three separate experiments. (B) The extent of scaffold protein immunoprecipitation was quantified by scanning densitometry. Data are the means ± S.E.M. from three separate experiments. (**) $P<0.01$ and (***) $P<0.001$.

Fig. 6. Assessment of receptor stimulated β-arrestin recruitment. Cells cotransfected with M_3^{Rluc} and β-arrestin^{GFP2} in presence or absence of 3ILoop minigene, were incubated for 20 min at various concentration of agonist or vehicle. The luciferase substrate DeepBluC coelenterazine was added immediately prior to BRET measurement. Data shown are means ±S.E.M of the five independent experiments.

TABLES

Table 1. Ligand binding properties of M_3 and M_5 mAChR constructs. Radioligand binding studies on HEK293T cell membranes expressing M_3 or M_5 wild type mAChR alone or together with the 3ILoopoop-minigene were carried out as described under *Materials and methods*. Curves were better fitted by non-linear regression analysis assuming a single binding site. K_D values were determined by using GraphPad Prism software. Results represent means ± S.E. (n = 5).

	[^{3}H]-NMS Binding	
Receptor construct	**K_D (pM)**	**B_{max} (fmol/mg)**
3 x HA-M_3	85.3 ± 17.7	1250 ± 106
3xHA-M_3 + 3ILoop	86.8 ± 27.9	1219 ± 66
3 x HA-M_5	164.9 ± 41.4	934 ± 45
3xHA-M_5 + 3ILoop	163.7 ± 55.3	908 ± 32

Fig. 1 Borroto-Escuela et al. 2009

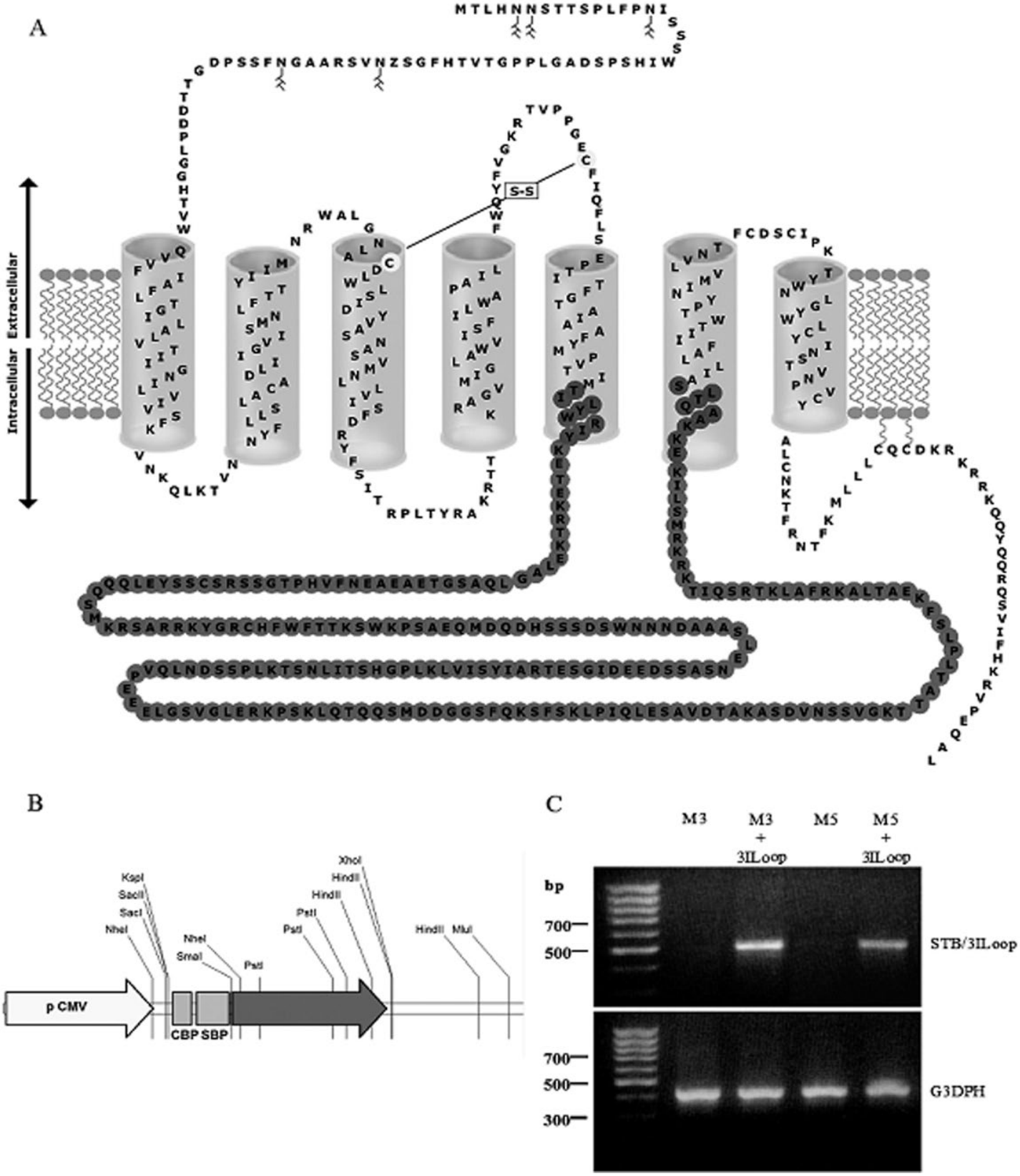

Fig. 2 Borroto-Escuela et al. 2009

A

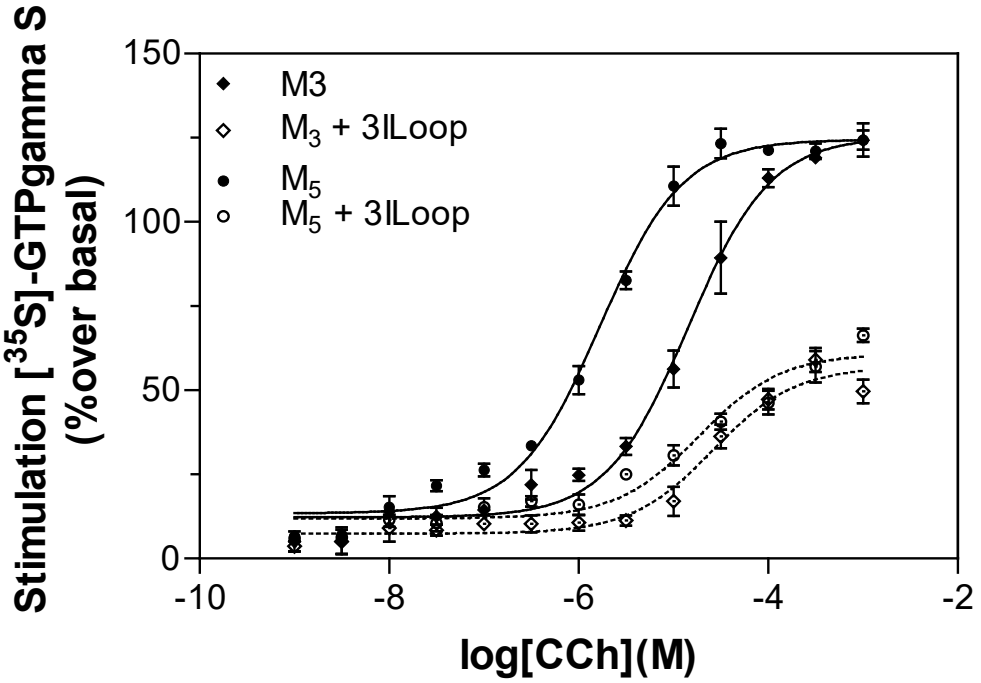

B

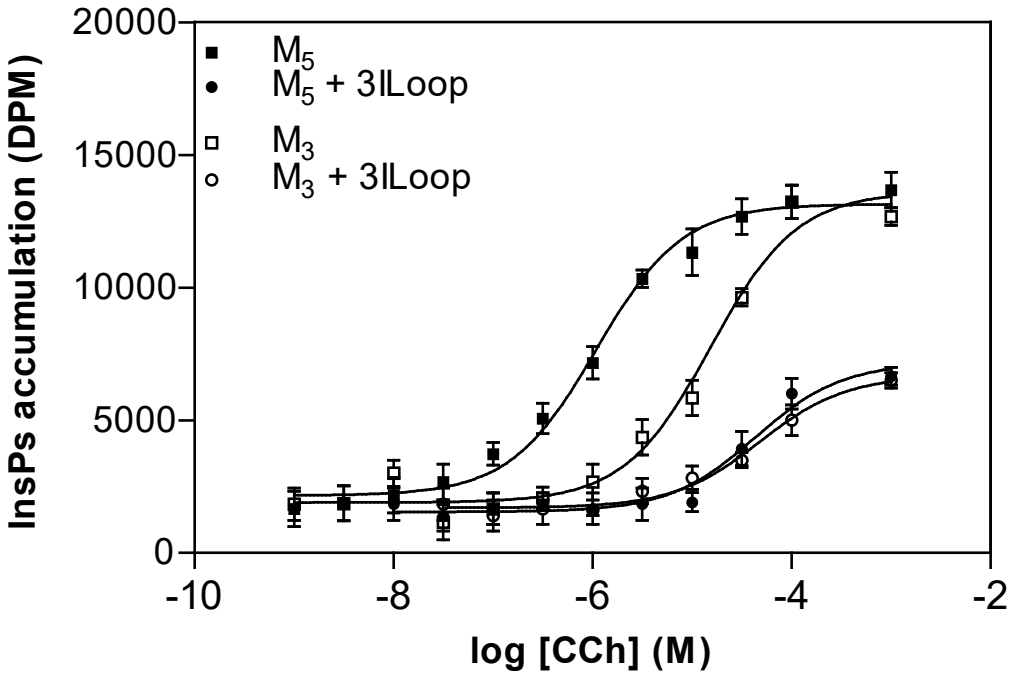

Fig. 3 Borroto-Escuela et al. 2009

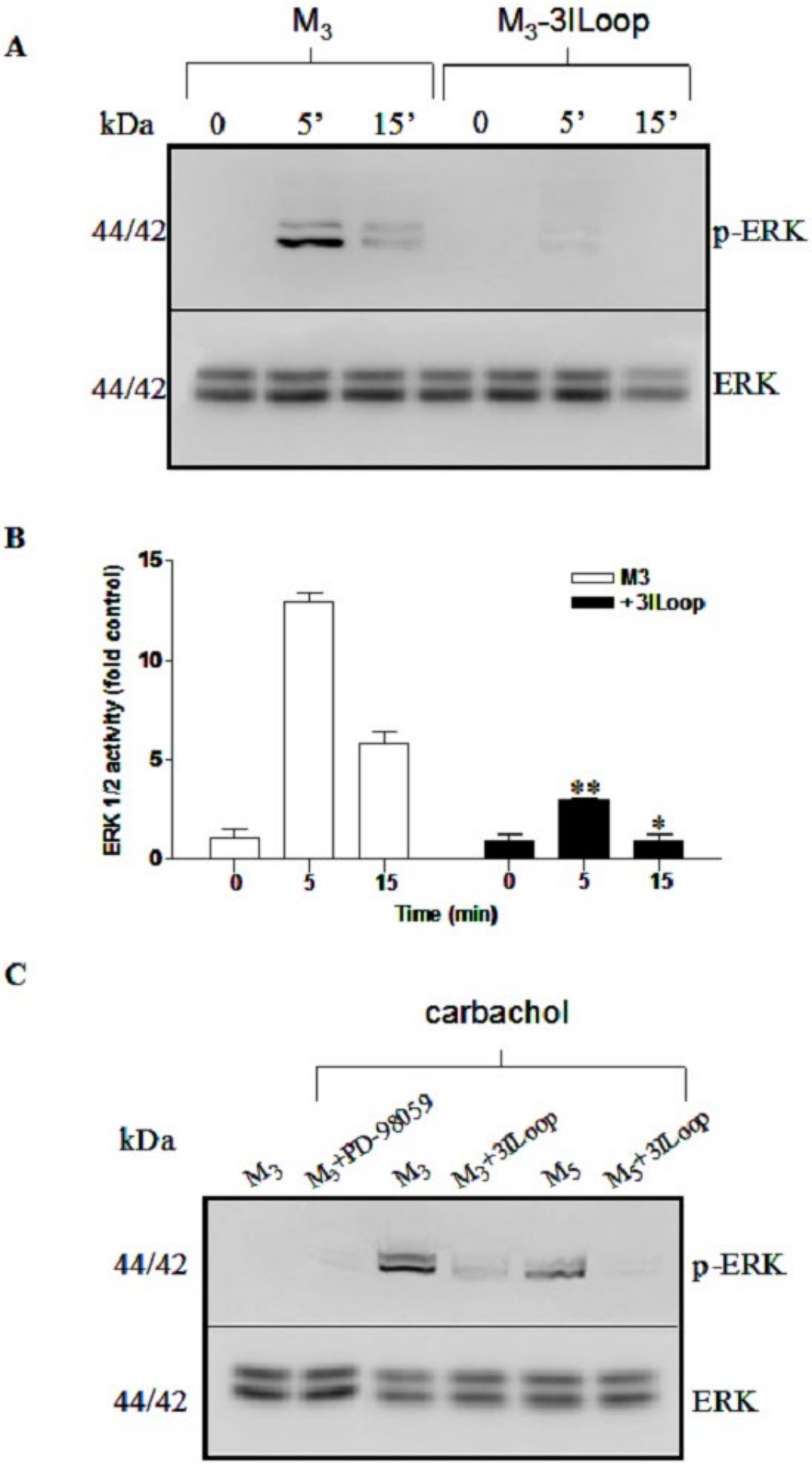

Fig. 4 Borroto-Escuela et al. 2009

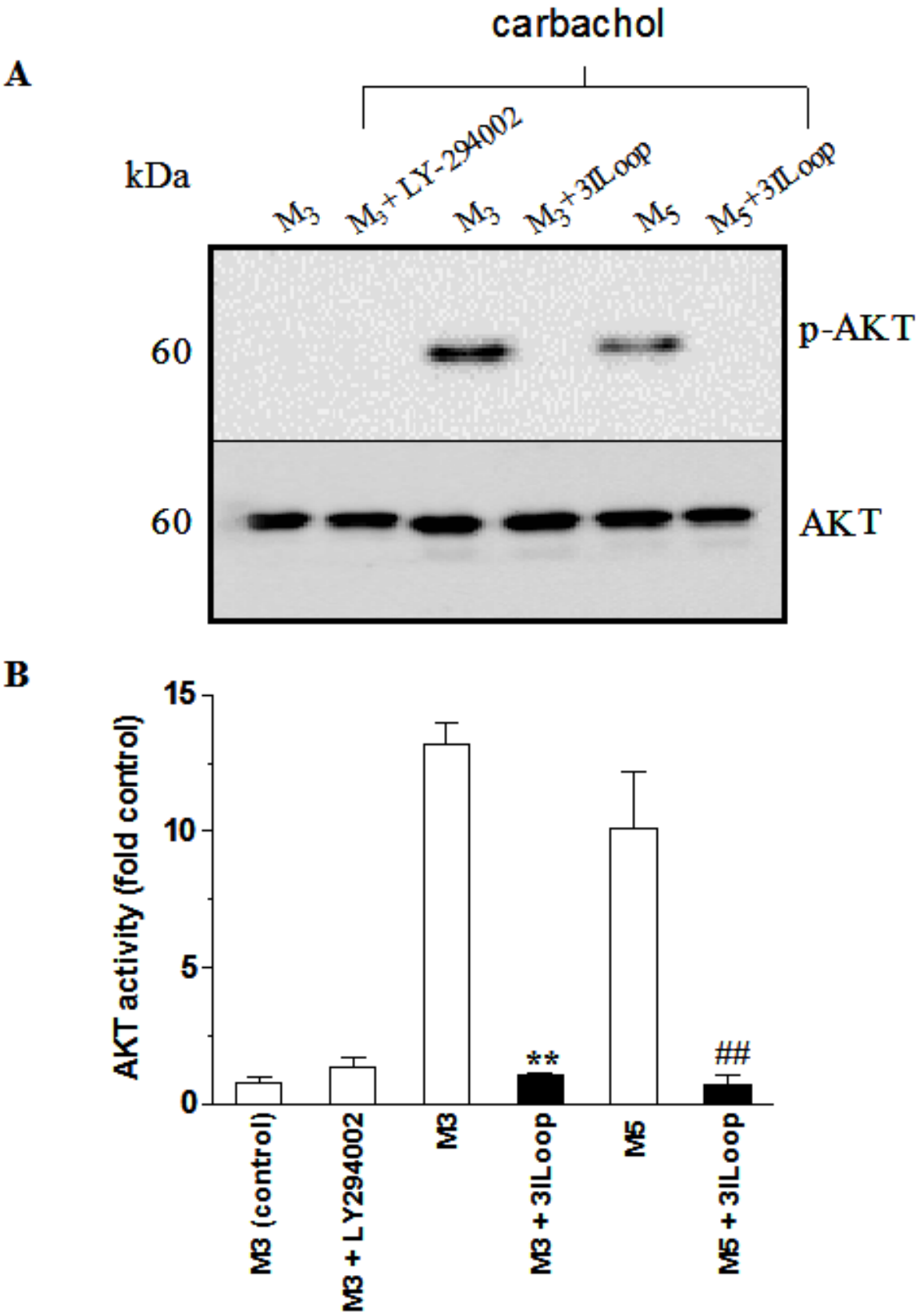

Fig. 5 Borroto-Escuela et al. 2009

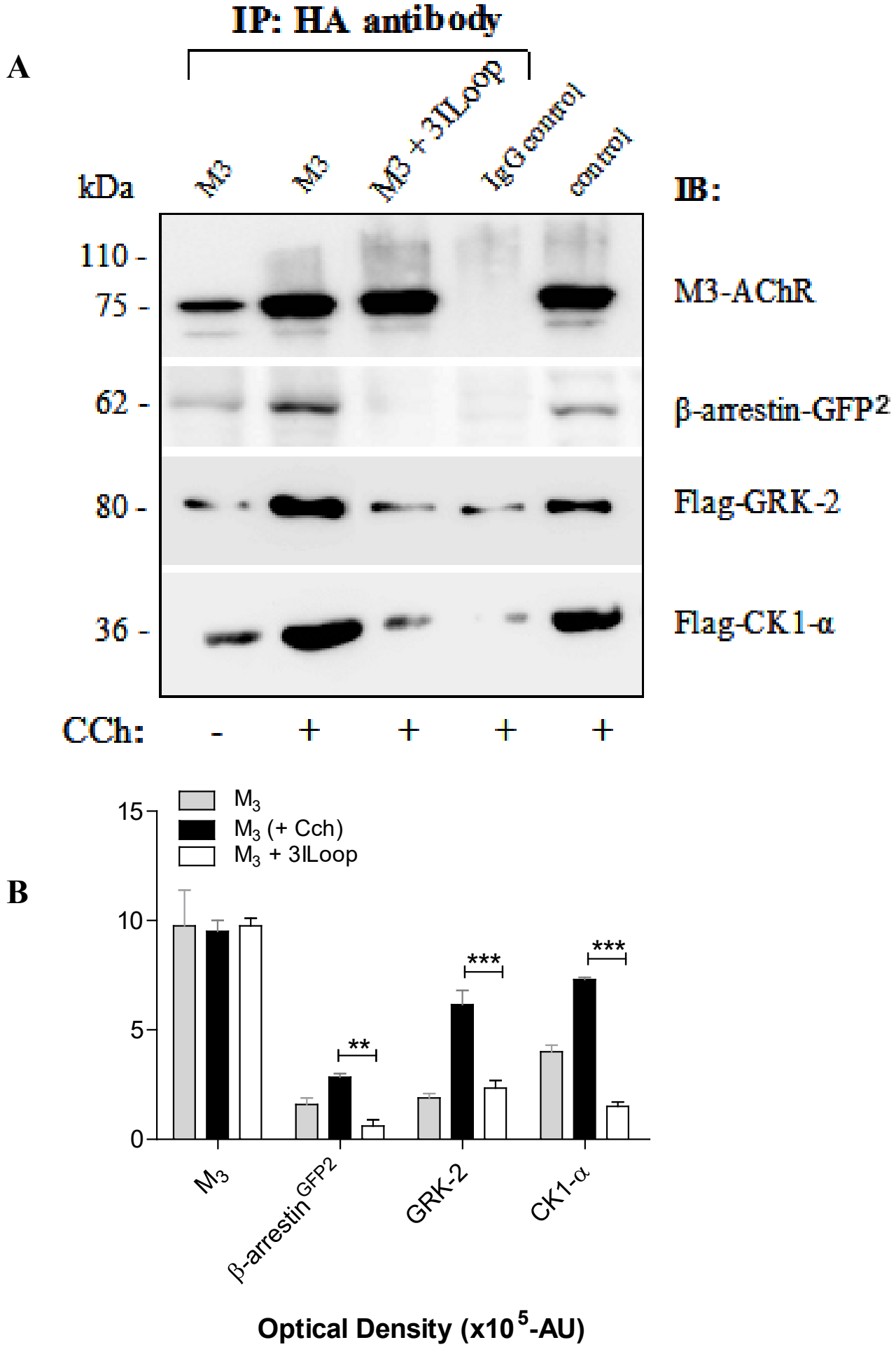

Fig. 6 Borroto-Escuela et al. 2009

A

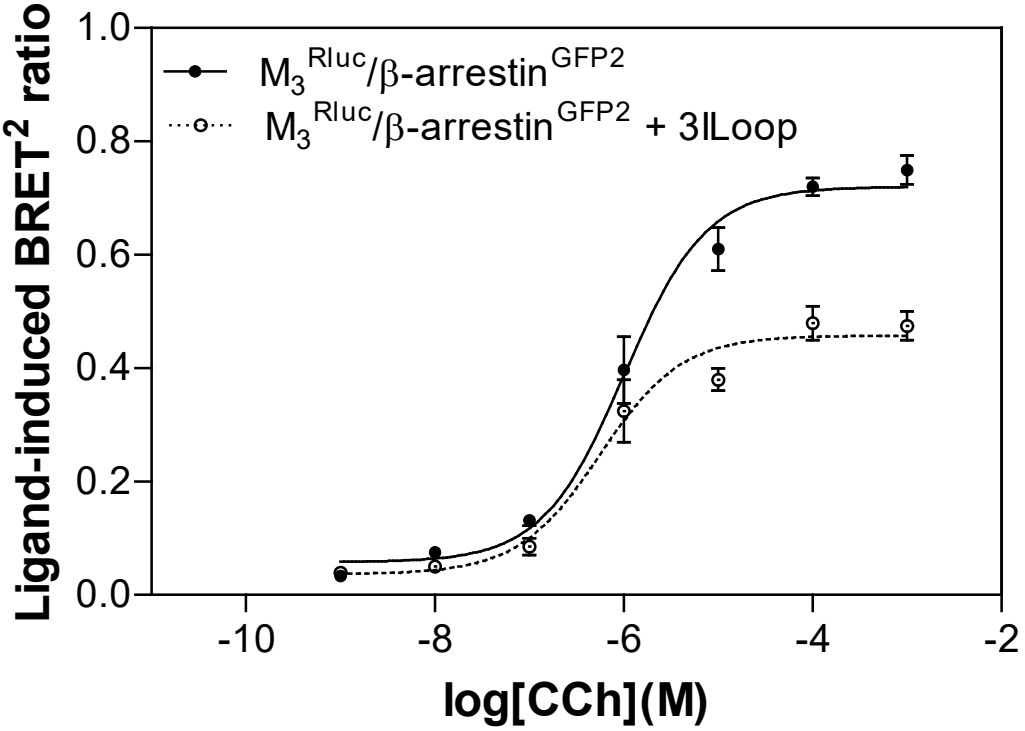

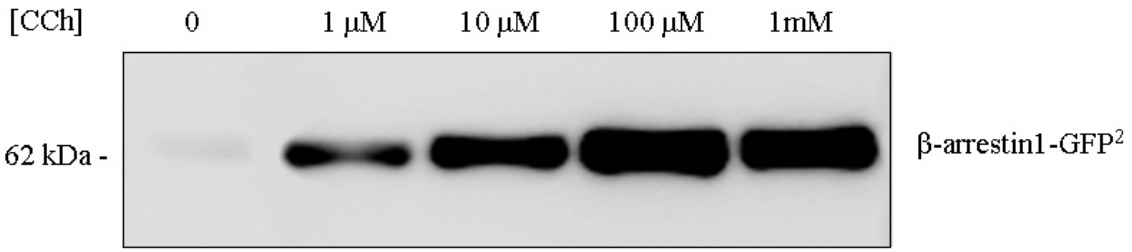

B **IP: anti-HA** **IB: anti-β-arrestin1**